Accepted Manuscript

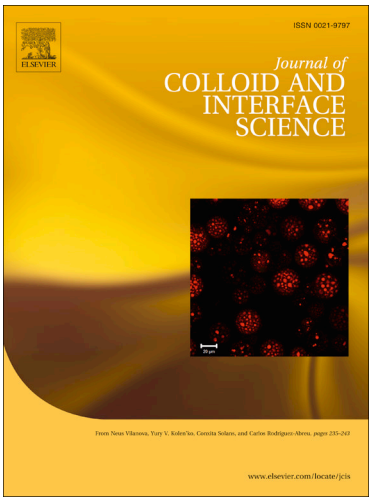

Regular Article

Sensitive and uniform detection using Surface-Enhanced Raman Scattering: Influence of colloidal- droplets evaporation based on Au-Ag alloy nanourchins

Dongjie Zhang, Jixiang Fang, Tao Li

PII: S0021-9797(17)31407-8
DOI: https://doi.org/10.1016/j.jcis.2017.12.017
Reference: YJCIS 23089

To appear in: *Journal of Colloid and Interface Science*

Received Date: 29 September 2017
Revised Date: 25 November 2017
Accepted Date: 5 December 2017

Please cite this article as: D. Zhang, J. Fang, T. Li, Sensitive and uniform detection using Surface-Enhanced Raman Scattering: Influence of colloidal- droplets evaporation based on Au-Ag alloy nanourchins, *Journal of Colloid and Interface Science* (2017), doi: https://doi.org/10.1016/j.jcis.2017.12.017

This is a PDF file of an unedited manuscript that has been accepted for publication. As a service to our customers we are providing this early version of the manuscript. The manuscript will undergo copyediting, typesetting, and review of the resulting proof before it is published in its final form. Please note that during the production process errors may be discovered which could affect the content, and all legal disclaimers that apply to the journal pertain.

ACCEPTED MANUSCRIPT

Sensitive and uniform detection using Surface-Enhanced Raman Scattering: Influence of colloidal- droplets evaporation based on Au-Ag alloy nanourchins

Dongjie Zhang [a], Jixiang Fang [a] and Tao Li [b]**

a. Key Laboratory of Physical Electronics and Devices of Ministry of Education, School of Electronic and Information Engineering, Xi'an Jiaotong University, Xi'an, Shaanxi, 710049, China.

b. Shaanxi Institute for Food and Drug Control, Xi'an, Shaanxi, 710065, China.

ABSTRACT: Surface Enhanced Raman Scattering (SERS) has been developed into a powerful vibrational spectroscopy technique for chemical detection. However, the fabrication of colloidal droplets-based SERS substrates with well reproducibility and uniformity still remains challenging. In this paper, colloidal suspensions of hollow Au-Ag alloy nanourchins (HAAA-NUs) and Au nanoparticles (Au NPs) with different morphologies were employed as SERS-active substrates. After evaporation of colloidal suspensions, we evaluated the SERS performance based on the following features: "Coffee Ring Effects", adsorption processes of probe molecule and colloidal NPs, spin coating and morphologies of suspended NPs. The results demonstrated that SERS signals could be enhanced enormously in the marginal region of "coffee ring" patterns. The limit of detection (LOD) for amaranth molecule would be reached 10^{-8} M. Moreover, by combining the droplets evaporation of HAAA-NUs suspensions with spin coating, the relative standard deviation (RSD) could be down to 3.5%,

ACCEPTED MANUSCRIPT

showing excellent reproducibility. The investigation here would provide a simple, practical and portable SERS detection method with excellent signal uniformity.

KEYWORDS: "Coffee Ring Effects"; Au-Ag alloy nanourchins; Adsorption process; SERS

INTRODUCTION

Since the discovery of SERS 40 years ago, this technique has attracted considerable attentions, due to the advantages of high sensitivity, effective selectivity and unique spectroscopic fingerprint. Being one of the most powerful vibrational spectroscopy techniques for non-destructive, on-site and in vivo analysis of chemical and biological substances,[1-6] SERS technique has been applied in various fields, such as electrochemistry,[7,8] catalysis,[9-11] biosensing,[12] food safety[13-15] and environmental monitoring.[16,17] As a relatively complicated system, SERS detection refers to the interactions between light and plasmonic nanostructures, probe molecule and light, as well as probe molecule and plasmonic nanostructures. Theoretical studies show that the electromagnetic enhancement effects, generated from the interaction of laser light and plasmonic nanostructures, would contribute to the SERS process for more than ~70% because of the localized surface plasmon resonances (LSPR). Therefore, the compositions, shapes, sizes and aggregations of plasmonic nanostructures (as shown in Table 1) would play critical role on the SERS performance.[18-26] Up to now, nanostructures with defined sizes, shapes and inter-particles space have been controlled precisely. Various SERS substrates with plenty of nanogaps, crevices or sharps have also been fabricated, exhibiting high density of "hot spots".

Table 1 Impact factors which influence the sensitivity, reproducibility, and stability of SERS signals

ACCEPTED MANUSCRIPT

Impact factors	SERS performance (Sensitivity, LOD, Reproducibility and Stability)
Compositions	Gold, silver or copper NPs, alloys or core-shell nanostructure, graphene, semiconductors，transition metal…
Shapes	Sphere, rod, polyhedron, star, urchins…
Aggregation	Dimers, Trimers, Aggregates, Arrays, 3D Superstructures, “Coffee ring effects”, Spin coating …
Sizes	Diameters, aspect ratio, distance of junctions …
Test condition	Laser wavelength, Laser power, Polarization direction, Integral times …
Probe molecules	Raman cross-section, Adsorption type, et al …

In fact, due to the simplicity of sample preparation, low cost and ultrasensitive detection, colloidal droplets-based SERS substrates have been studied widely. However, the aggregations of colloidal NPs after solvent evaporation exhibit various patterns. Due to the well-known “coffee ring effects”, uneven distribution of species would be obtained, which is mainly responsible for the uncontrolled SERS uniformity and reproducibility.[18-20] Therefore, a better understanding and controlling of the drying process of colloidal suspensions is helpful to realize a uniform SERS detection. Shao’ group[21] has obtained large-scale and uniform gold nanoparticle aggregates by a simple capillarity-assisted method, which could suppress the influence of “coffee ring effects” in a large extent. This SERS substrate exhibited high reproducibility and large Raman enhancement factors of 3×10^{10} for R6G molecule at 10^{-10} M. In our previous experiments[22], a flat film of hollow HAAA-NUs was fabricated by a simple double-sided tape assisted transfer method. The closely-packed aggregates of HAAA-NUs were formed on a Si support by reverse the top/bottom surface of evaporated layer with a

ACCEPTED MANUSCRIPT

common double -sided tap. The RSD of SERS signal could be less than 15%, showing excellent uniformity.

In addition, the absorption feature between the molecules of interest and plasmonic nanostructures is also important for SERS sensitivity and uniformity. Different adsorption processes, such as emerging the colloidal NPs into the analytical solutions or dropping the probe molecule onto the surface of prefabricated nanostructure patterns, would make great changes to the final SERS performance. Liao' group[23] found that SERS intensity strongly depends on the adsorbent location of probe molecules. If most of probe molecules were located at regions with "hot-spots", more sensitive Raman signal could be acquired. Otherwise, the SERS intensity of the probe molecules would be too weak to be detectable.

Here, different preparation processes of SERS substrates based on the evaporation of colloidal NPs were studied. The effects of "coffee ring" patterns, absorption processes of colloidal suspensions and analytes, shapes and sizes of NPs, and the spin coating were evaluated based on SERS sensitivity and reproducibility. As a result, SERS signals with excellent intensity and uniformity were obtained due to the uniform distribution of colloidal NPs and enhanced absorption capacity between the HAAA-NUs and analytes.

EXPERIMENTAL SECTION

Materials. Gold (III) chloride hydrate ($HAuCl_4 \cdot 4H_2O$, 99.999%), Trisodium citrate dehydrate ($Na_3C_6H_5O_7 \cdot 2H_2O$) 99+%, silver nitrate ($AgNO_3$) $\geqslant$ 90%, L-Dopa (3,4-dihydroxyphenylalanine) 98%, Ammonia solution ($NH_3.H_2O$, $\geqslant$25%), Formic acid (HCOOH, 98%) were purchased from Sigma Aldrich. Amaranth sample was received from

ACCEPTED MANUSCRIPT

Shaanxi Institute for Food and Drug Control. All chemical reagents were used without any purification. Water used throughout the synthesis was Ultrapure DI (18.2 MΩ, Millipore).

Synthesis of Au NPs with smooth surface (AuNSS). Spherical gold NPs were synthesized with a modified citrate reduction approach.[24] In a typical procedure, 100 mL aqueous $HAuCl_4$ (0.2 mM) was put into a 250 mL three-neck flat-bottom flask. After the solution was boiled, 2 mL sodium citrate solution (0.01M) was added with stirring (300 rpm). The solution became wine red in color after 1 h. The gold NPs were obtained by cooling down to room temperature.

Synthesis of Au NPs with rough surface (AuNRS) and HAAA-NUs. Gold NPs with rough surface were obtained by a seed-mediated synthesis method with no surfactants. The AuNSS above were used as gold seeds. A volume of 10 mL aqueous solutions (0.5 mM $HAuCl_4$ and 2 mL gold seeds) was prepared in a 25 mL glass vial. Then, 2 mL L-DOPA solution (0.01M) was added quickly by a 5 mL pipette. After 10 min, the products were collected by centrifugation at 5000 rpm for 10 min, and then were washed with HCOOH once, and DI water twice. Finally, 60 nm sized AuNRS were obtained. In addition, the HAAA-NUs suspensions were prepared by a typical method our laboratory reported before.[25]

ACCEPTED MANUSCRIPT

ACCEPTED MANUSCRIPT

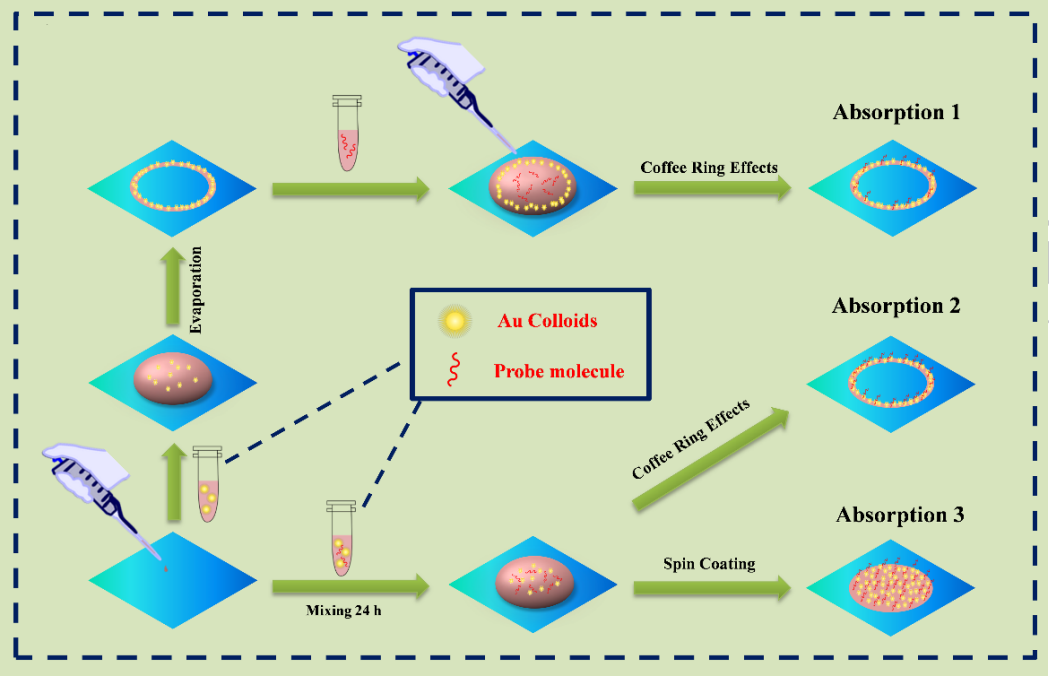

Figure 1 Schematic of the preparation process of SERS-active substrates based on colloidal-droplets evaporation.

Preparation of SERS Substrates. Three kinds of colloidal NPs were employed as SERS substrates. Silicon wafer was used as the supporter, rinsing with aqua regia once, DI water twice and ethanol twice under ultrasonic condition. As a common dye molecule added in fruit juices and wines, amaranth was chosen to be the probe molecule. Fig 1 illustrated the preparation process of SERS-active substrates based on the evaporation of colloidal droplets. Three kinds of adsorption processes for HAAA-NUs NPs and probe molecules were employed. For Absorption 1, 30 μL colloidal suspensions were dropped on Si substrates, and "coffee ring" patterns appeared during the evaporation process. Then, 50 μL amaranth aqueous solutions with various concentrations were added, insuring the coverage of "coffee ring" patterns. Moreover, the concentrations of gold NPs could be adjusted for getting different "coffee ring" patterns. For Absorption 2, gold NPs and the analytes were mixed for 24 h firstly before dropping onto a surface. Then, 50 μL mixed solutions were dropped on the Si substrate, and thus SERS substrates were obtained after the evaporation of solvent. In order to obtain more uniform dispersed SERS substrates, spin coating was employed during

ACCEPTED MANUSCRIPT

the evaporation process of mixed colloidal NPs and analytes in absorption 2. This method was defined as Absorption 3. The rotate speed was 1000 rpm, and duration time was 40s. All the samples were dried overnight, and then three kinds of SERS substrates were obtained.

Characterization. The distributions, sizes and morphologies of synthesized colloidal NPs were characterized by a Scanning electron microscope (SEM, JSM-7000F) at an accelerating voltage of 20 kV. Transmission electron microscopy (TEM, JEM-2100, JEOL) was performed with the microscope operating at 200 kV. The concentrations of HAAA-NUs colloids were measured by ICP-MS (NexIONTM 350D，PerkinElmer (PE)). The RF Power was 1100W. Nebulizer Gas Flow was 0.90L/min. Plasma Gas Flow was 16.0L/min, and the Integration Time was 5s. SERS measurements were conducted on a portable Raman system (BWTEK, i-RAMAN plus) with a 785 nm laser. A confocal microscope was used to focus the laser with a 100X objective and 10s for exposure time. The laser power was 10% (about 30 mW). The SERS signals were collected at the different areas of “coffee ring” patterns.

RESULTS AND DISCUSSION

As the SEM image shown in Fig 2(a), colloidal HAAA-NUs prepared by a seed-mediated growth method displayed high density of sharp tips with tens of nanometers. During the SERS test, these tips may serve as nanoantennas, and the nanogaps of abundant tips may provide ultrahigh density of “hot spots”. Fig 2(b) demonstrated that the HAAA-NUs possessed excellent uniformity in shape and size. Many studies have shown that Au-Ag alloy may have better SERS performance, compared with pure Au nanostructures. Moreover, the HAAA-NUs with well chemical stability will improve the reliability of SERS substrates.

ACCEPTED MANUSCRIPT

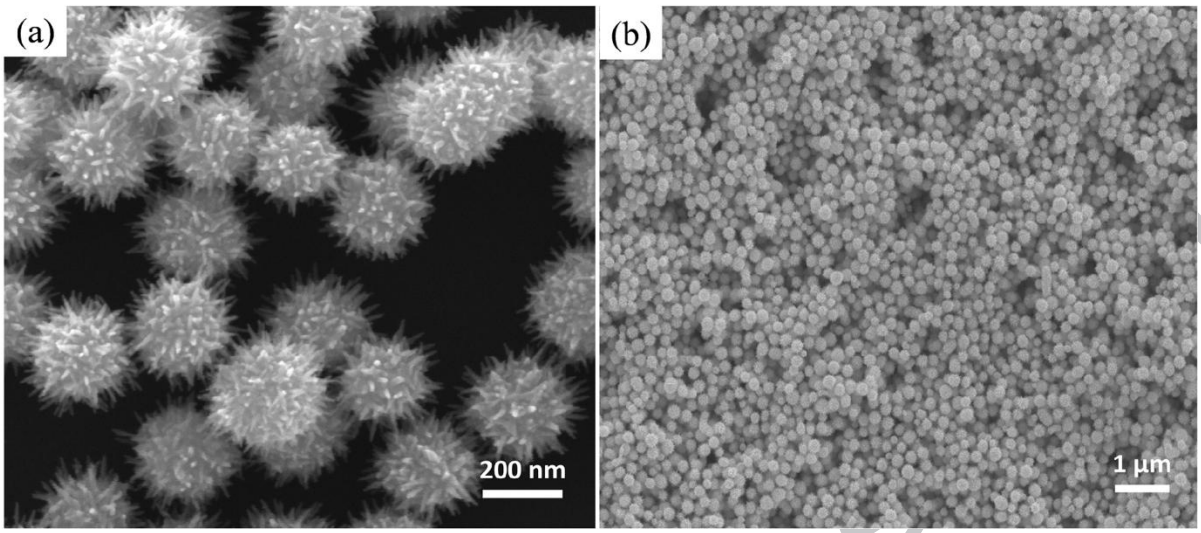

Figure 2 SEM images of the HAAA-Nus with various resolutions: (a) high magnification; (b) low magnification

Here, the initial concentration of HAAA-NUs suspension without any dilution was defined C_1. Therefore, C_2 and C_3 were meant that the colloidal HAAA-NUs were diluted for 2 and 4 times, respectively. As a result, the experimental data obtained from ICP-MS showed that the values of C_1, C_2 and C_3 were 216、142 and 63.6 ppm, respectively.

"Coffee Ring Effects" with HAAA-NUs suspensions

"Coffee-ring effects" refers to the accumulation of a ring-like dense array on the border by the evaporation of droplets on solid surfaces. In this process, three-phase contact line among the atmosphere, droplet and solid substrate is pinned. A remarkable capillary flow happens because of the evaporation of solvents, driving solutes to move outward from the inner side to the rim of the droplet. Consequently, solutes are highly concentrated along the original droplet edge. The studies showed that "coffee-ring effects" could be applicable for enriching the probe molecules and NPs, resulting in a huge enhancement of SERS signal.[26]

ACCEPTED MANUSCRIPT

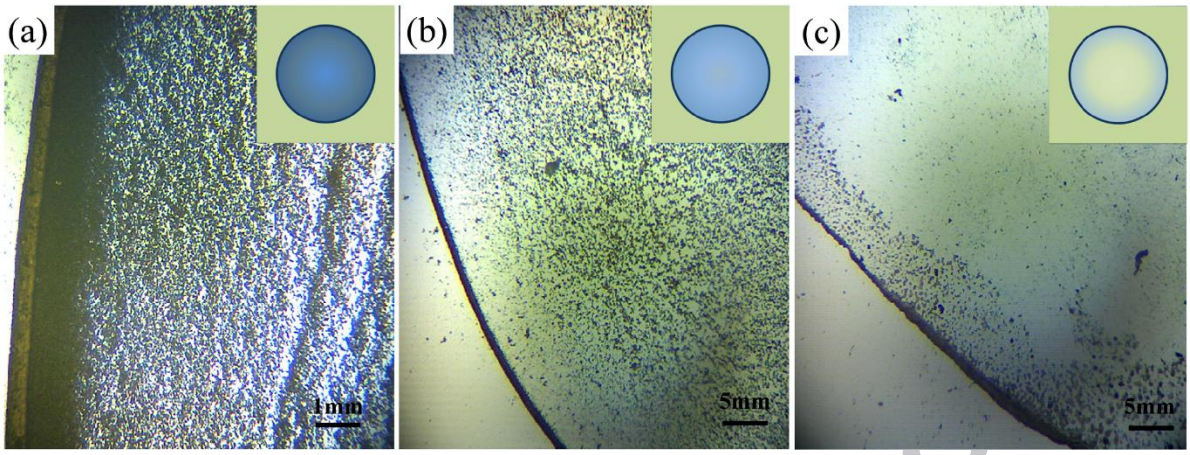

Figure 3 Optical images of different "coffee rings" patterns, prepared with various concentrations of HAAA-NUs: (a) C_1; (b) C_2; (c) C_3. The insets were the sketch maps of "coffee rings" patterns deposited on silicon wafer.

The "coffee-ring" patterns showed strong dependence on the concentration of colloidal NPs. Due to the capillary flow and pinned contact line during solvent evaporation[27], different shapes of "coffee-ring" patterns were obtained for various concentrations of colloidal NPs based on Absorption 1, as shown in Fig 3. When colloidal HAAA-NUs with C_1 were dried, the density of NPs was extremely high for either the marginal or central region. However, for the HAAA-NUs with concentration C_2, colloidal NPs were concentrated in the marginal area, and the distribution of the SERS substrate was thin obviously at the center. When the concentration of HAAA-NUs was diluted to C_3, few amounts of nanoparticles assembling in central region was formed, as could be seen in Fig 3(c). The insets in Fig 3 and Fig S1 showed the patterns of intact "coffee rings", which were in accordance with the distribution features of colloidal HAAA-Nus. .

In order to study the SERS properties of colloidal HAAA-NUs, amaranth at concentration of 10^{-6} M was utilized as probe molecules. SERS spectra in Fig 4 (a) shows the major vibrational peaks of amaranth at 942, 1060, 1180, 1233, 1346, 1365, 1483, 1516, and 1575 cm^{-1}, respectively. The peaks at 942 cm^{-1} were caused by the stretching vibrations of C-S and

ACCEPTED MANUSCRIPT

C-O-C bonds, respectively. The peaks at 1054 cm^{-1} and 1180 cm^{-1} were due to the bending and swing of CH_2. The band at 1235 cm^{-1} was related to the aromatic vibrations, and peaks at 1346 cm^{-1}, 1365 $cm^{-1}$and 1483 cm-1 were due to the C-H deformation vibrations. The peaks at 1516 cm^{-1} and 1575 cm^{-1} were attributable to the aromatic stretching vibrations.

Raman spectra of ten spots (red dots marked in the insets) were acquired randomly in the marginal and central regions of "coffee ring" patterns, respectively, as shown in Fig S2. The reproducibility of SERS performance was evaluated based on the scattered points. Owning to the excellent SERS activity of HAAA-NUs, the spectra of each collected spot clearly show the characteristic Raman peaks of amaranth with a low concentration (10^{-6} M) even though that the HAAA-NUs was diluted to concentration C_3 (Fig S2(e) and S2(f)). In the case of "coffee ring effects", an enhancement occurred from central regions to marginal regions. Moreover, it is obvious that the SERS signals showed a better uniformity in the marginal area of "coffee ring" patterns rather than the central area.

To assess the SERS performance of HAAA-NUs in detail, the representative bands at 1365 cm^{-1} and 1516 cm^{-1} were chosen to investigate the marginal regions and central regions of "coffee ring" patterns. The average signal intensities (I_{ave}) at these two bands were measured, and the values of relative standard deviation (RSD) were calculated according to the intensities of SERS signals. The values of I_{ave} and RSD for various SERS substrates were summarized in Table S1. The results indicated that the SERS performance showed strong dependence on the distribution and density of HAAA-NUs particles.

ACCEPTED MANUSCRIPT

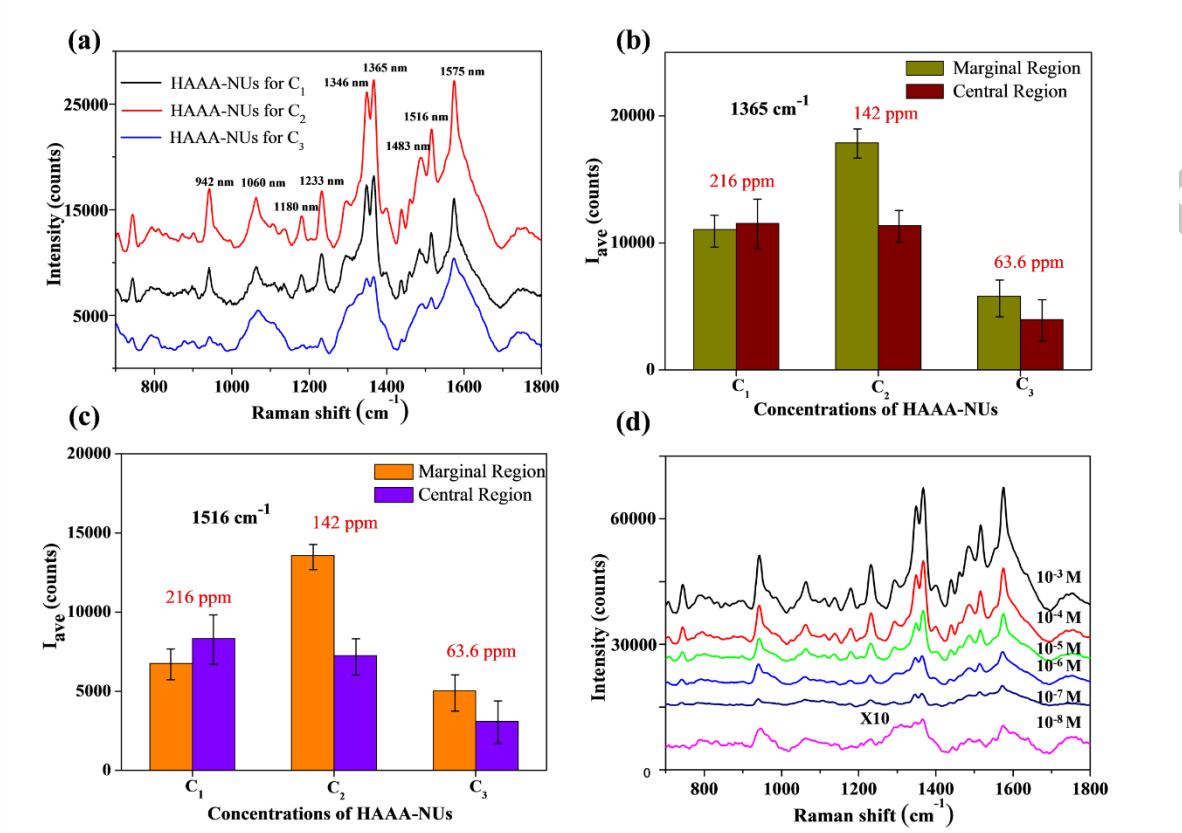

Figure 4 SERS spectra of 10^{-6} M amaranth for different "coffee rings" patterns: (a) SERS signal intensities with various HAAA-Nus concentrations in marginal region; (b) and (c): Contrast of I_{ave} with various HAAA-NUs concentrations. (d) SERS spectra of amaranth with different concentrations. The fabrication of SRES substrates were all based on Absorption 1. The exposure time was 10s, and the laser power was 30 mW

Fig 4 (a) illustrated representative SERS spectra with various HAAA-NUs concentrations, which indicated that the SERS signal was more sensitive with the condition of concentration C_2. Fig 4 (b) contrasted the value of I_{ave} for various concentrations of HAAA-NUs suspensions in different "coffee ring" regions. As for 1365 cm^{-1} band, the results confirmed that the SERS signal in marginal region was more sensitive for concentration C_2 and C_3. However, for concentration C_1, the date indicated that I_{ave} in central region was little stronger than that of outer area, which might be ascribed to the excessive aggregation of the HAAA-NUs in the marginal section of "coffee ring". Also, the data in Fig 4(c) showed the same phenomenon for 1516 cm^{-1} band.

ACCEPTED MANUSCRIPT

Moreover, an interesting phenomenon occurred that the I_{ave} received an obvious enhancement, when the concentration of HAAA-NUs reduced from C_1 to C_2. We could clearly found that the most insensitive Raman intensity was obtained with concentration C_2. In the marginal regions, the I_{ave} values were about 11056, 17868 and 5809 counts for concentration C_1, C_2 and C_3, respectively. Fig 4(c) also confirmed the above results at 1516 cm^{-1} band. When the concentration of HAAA-NUs was too high, the produced "hot-spots" would not be more enormous. Due to the aggregation of NPs in the vertical direction, it may lead to the piling up of colloidal NPs and the elimination of "hot-spots"[23]. So, the density of SERS-active NPs was not the higher the better, at least for the HAAA-NUs. However, when more diluted colloidal HAAA-NUs (C_3) were employed for SERS analysis, the RSD and average intensities of SERS signal were declined in a certain extend, as could be seen in Fig S2(e) and S2(f), exhibiting poor SERS reproducibility and sensitivity. The reason could be attributed to uneven distribution and reduced SERS "hot spots" with low concentrated HAAA-NUs particles. When the concentration of HAAA-NUs was C_2, the RSD values were 11.38% and 12.73% in the marginal region, and 17.87% and 18.75% in the central area, for the bands of 1365 cm^{-1} and 1516 cm^{-1}, showing a better SERS signal uniformity compared to other "coffee ring" patterns. The RSD values in Table S1 also confirmed the result for various concentrations of colloidal HAAA-NUs.

The potential application of colloidal droplets-based SERS substrates for ultrasensitive detection of amaranth was studied. We measured the SERS spectra of amaranth with a series of concentrations (10^{-3} M to 10^{-8} M), and the SERS signal was collected with concentration C_2, and the detection area was located at the margin regions of "coffee ring" patterns. The spectra in Fig 4(d) clearly showed the characteristic Raman peaks of amaranth even at a concentration as low as 10^{-7} M. The reported lowest concentration was 10^{-6} M in literature.[28,29] Moreover, when the concentration was down to 10^{-8} M, SERS signal could be still recognized by amplification of SERS intensity 10 times, indicating that the LOD was much lower than

ACCEPTED MANUSCRIPT

the technique performance limit (0.05g/kg) required by the Chinese Hygienic standard for food additives. These colloidal HAAA-NUs were sensitive enough to detect amaranth in practice.

Different adsorption process in HAAA-NUs system

We all know that water exhibits extremely weak SERS signal intensities due to the relatively small Raman cross-section. For water-soluble probe molecules, the SERS behavior would be influenced by the ability to absorb behavior to the specific enhancing surface.[30] In order to investigate the effects of absorption process, the aqueous HAAA-NUs solution was mixed with probe molecule for 24 h in dark. Compared with the above-mentioned process, Absorption 2 would allow a sufficient physical and chemical adsorption between the HAAA-NUs and amaranth molecules. The concentration was C_2. After the mixing step, 50 μL mixed solution was dripped onto the cleaned silicon wafer. During the evaporation of water, HAAA-NUs and probe molecules would migrate from the inner solution to the edge of three-phase contact line among the droplet, silicon surface and air. After several minutes, densely packed HAAA-NUs and concentrated analytic molecules were deposited on the contact line, which would be used for the SERS detection.

ACCEPTED MANUSCRIPT

ACCEPTED MANUSCRIPT

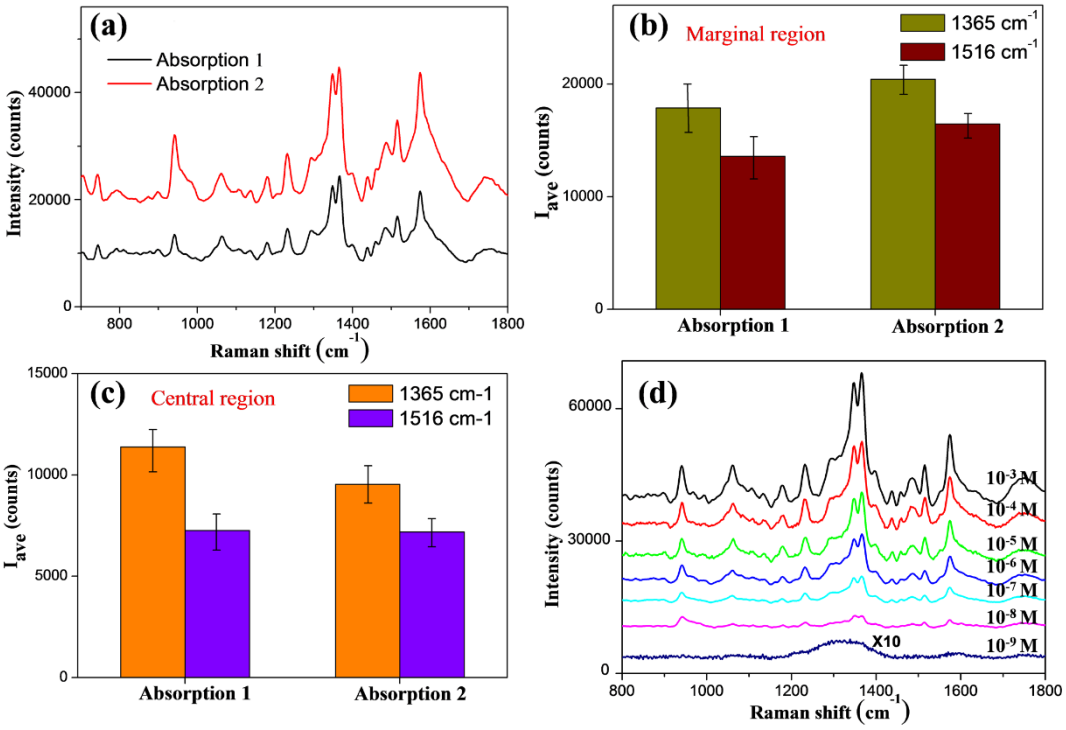

Figure 5 SERS spectra of 10^{-6} M amaranth with the process of Absorption 2. (a) Contrast of different absorption types; (b) and (c): SERS signal intensities for different "coffee rings" region; (d) SERS spectra of amaranth with different concentrations. The HAAA-Nus concentration was C_2. All measured conditions were same as process of Absorption 1

For the process of Absorption 2, Fig S3 (a) and (b) showed the SERS spectra of 10^{-6} M amaranth in the marginal area and central area of "coffee ring", respectively. The insets were the optical images of the "coffee ring" patterns. As shown in Figure 5 (a), compared to the process of Absorption 1, the intensity of SERS signals with Absorption 2 obtained a huge enhancement. Figure 5 (b) and 5(c) contrasted the SERS signal intensities for different "coffee rings" region. The average intensities of marginal region at 1365 cm^{-1} was 20433, and 1516 cm^{-1} for 16466, whereas the bands at 1365 cm^{-1} was 9533, and 1516 cm^{-1} for 7176 for the central region. In addition, Table S1 indicated that the values of RSD in marginal region were 7.78% for 1365 cm^{-1} and 5.47% for 1516 cm^{-1}, showing excellent reproducibility. The data here at least matches and probably exceeds that of the best colloidal substrates (<10%).[31]

ACCEPTED MANUSCRIPT

Even though in the central area, the RSD values of 1365 cm^{-1} and 1516 cm^{-1} could also be reached for 18.07% for and 11.35%, respectively.

The excellent reproducibility and enhanced signal intensity may be ascribed to the increased molecules located at the junctions between adjacent gold tips or NPs. The enhanced electromagnetic fields generated from the excitation of LSPR could act as an optical trap for the probe molecule and thus produce huge SERS signals.[32,33] In addition, more amaranth molecules would be adsorbed on the roughened surface of HAAA-Nus with the prolonged mixture. Charge-transfer phenomenon might be appeared between the noble metal and adsorbed molecules, which would generate the chemical enhancement of SERS signal.[34,35]

Based on the excellent intensity and reproducibility of SERS signal, the LOD of amaranth was also be evaluated. Raman spectra was collected in the same condition shown in Fig 4. As shown in Fig. 5 (d), Raman spectra of amaranth molecules at different concentrations from 10^{-3} M to 10^{-9} M was investigated. The LOD concentration of amaranth could be reached to 10^{-8} M. Even at the concentration down to 10^{-8} M, all of the Raman peaks could be still well recognized. However, with the first adsorption type, a few main Raman bands were acquired by the amplification of SERS intensity 10 times. The results showed that the absorption type of probe molecules with sensitive HAAA-NUs played an important role on the sensitivity and LOD of SERS signal. This may be attributed to the increased molecules in the enhanced electromagnetic fields and chemical enhancement mentioned above. In addition to the prolonged test time, this method would provide a more sensitive and uniform SERS detection platform for various target analytes.

Influences of colloidal morphologies

In order to study the influences of “coffee ring effects”, gold NPs with various shapes were chosen as the active SERS substrates. Contrast to HAAA-NUs, AuNRS was prepared () by a

ACCEPTED MANUSCRIPT

seed-mediated growth method. As shown in Fig 6(a), the synthetic sample has narrow size distribution with 60 nm around. What's more, the embossments on the nanoparticle surface may contribute to a great electromagnetic enhancement, which may provide well SERS behavior.

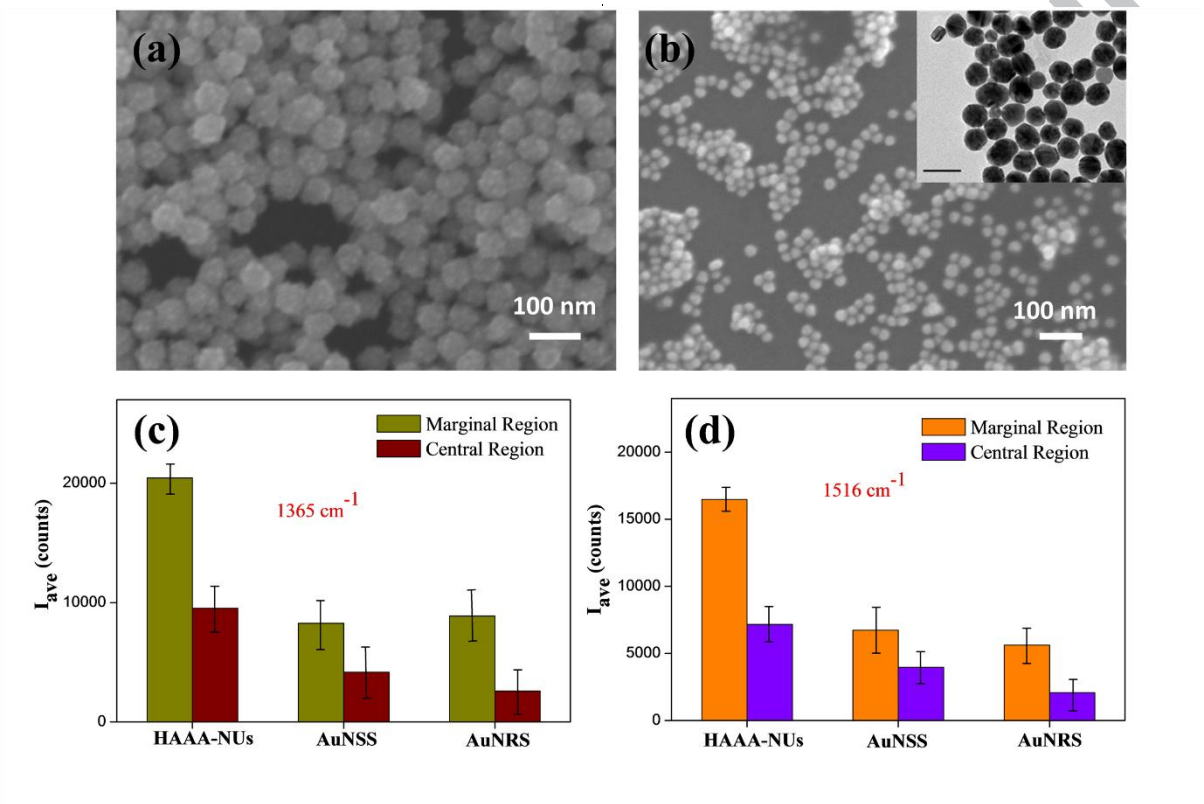

Figure 6 SERS spectra of 10^{-6} M amaranth based on various colloidal NPs. (a) SEM images of AuNRS; (b) SEM images of AuNSS. (c) and (d) SERS signal intensities for different substrates. The inset in (b) was TEM image, the scale bar was 50 nm.

In addition, Fig 6(b) showed the SEM images of gold NPs with smooth surface (AuNSS). The average size was centered at approximately 40 nm. The inset in Fig 6 (b) was the TEM image of AuNSS, being in accordance with the general size of Au NPs. It was worth noting that the gold NPs here had a spherical shape with smooth surface, and possessed a relatively uniform size distribution.

ACCEPTED MANUSCRIPT

For the preparation of SERS substrates, the colloidal AuNRS and AuNSS were mixed with probe molecule for 24 h firstly, and then were dripped onto silicon wafer. After evaporation of water, the "coffee ring" patterns were also emerged. The SERS sensitivity, LOD and reproducibility were measured. For AuNRS and AuNSS, the lowest detection concentration of amaranth was 10^{-7} M, showing an obvious decline compared with the HAAA-NUs above. This may ascribed to the absence of nanosharps and junctions. Figure S4 and S5 showed the SERS spectra of 10^{-6} M amaranth for AuNRS and AuNSS, respectively. For colloidal AuNRS substrate, the values of RSD in the marginal region were 14.65% for 1365 cm^{-1} and 19.49% for 1516 cm^{-1}, showing well performance of reproducibility. In the central area of coffee ring, the RSD values of 1365 cm^{-1} and 1516 cm^{-1} were 27.3% for and 12.84%, respectively. The results verified that SERS reproducibility in marginal region of "coffee ring" was better than that of central region. Besides, the average intensities of marginal region at 1365 cm^{-1} was 8263, and 1516 cm^{-1} for 6722, whereas the bands at 1365 cm^{-1} was 4180, and 1516 cm^{-1} for 3964 for the central region.

For colloidal AuNSS substrate, the "coffee ring" pattern showed a significant difference with the HAAA-NUs and AuNRS. Almost all of the gold NPs were deposited in the margin area of "coffee ring". Time competition between the solute movement and solvent evaporation in droplet was important to the depositing morphology of different droplets.[36-38] During the evaporation process of sphere gold NPs, the outward capillary flow happened in the early stage, and the solute movement rate was much faster than the solvent evaporation rate. With the shrinking of droplet size, the solvent would be dried out slowly and therefore provide enough time for shifting the solute to the margin of droplets. Moreover, the values of RSD in the marginal region were 19.87% for 1365 cm^{-1} and 13.61% for 1516 cm^{-1}, showing a good reproducibility. The average intensities of marginal region at 1365 cm^{-1} was 8873, and 1516 cm^{-1} for 5628. However, the SERS intensity was very low in the central area. So, we prolonged the exposure time to 60s. As a result, the RSD values of 1365 cm^{-1} and 1516 cm^{-1}

ACCEPTED MANUSCRIPT

were 24.29% for and 22.64%, respectively. The average intensity at 1365 cm^{-1} band was 2598, and 1516 cm^{-1} band for 2070, respectively.

At last, Fig 6 (c) and 6(d) compared SERS signal intensities for different colloidal NPs. Contrast to AuNRS, the AuNSS substrate showed more sensitive SERS signal in marginal region of "coffee ring" pattern. Moreover, the colloidal HAAA-NUs substrates showed the most excellent SERS performance among these three shapes of NPs, whether in marginal or central regions.

Influences of Spin Coating in HAAA-NUs system

In order to receive more uniform and reproducible SERS signals, homogenous nanoparticle deposition during the colloidal droplets-evaporation was necessary. Recent researches had been devoted to presenting or suppressing the "coffee-ring effect" by adjusting the morphology and surface properties of NPs,[39-41] type of surfactants,[42-44] and substrates. However, the controlling of "coffee-ring effects" in evaporation process was difficult because many factors would affect the nanoparticle deposition, for instance, nanoparticle–nanoparticle interaction, nanoparticle–suspension interaction, and droplet–substrate interaction.[45,46] Therefore, a method to totally suppress the "coffee-ring effect" is highly required in order to acquire uniform self-assembly of NPs.

Here, we employ a simple and efficient method to control the NPs deposition against the "coffee ring" effects by using spin coating technique. As consequence of Absorption 3, a monolayer of HAAA-NUs NPs with probe molecules was obtained by the adjustment of spinning parameter, such as rotating speeds and times. It was worth noting that the pre-treatment of the supporting substrates was vital for the formation of HAAA-NUs layer. The silicon wafer should be hydrophilic by washing in turn with ethanol, acetone, H_2SO_4:H_2O_2 (3:1), H2O:NH_3•H_2O:H_2O_2 (5:1:1), and deionized water.

ACCEPTED MANUSCRIPT

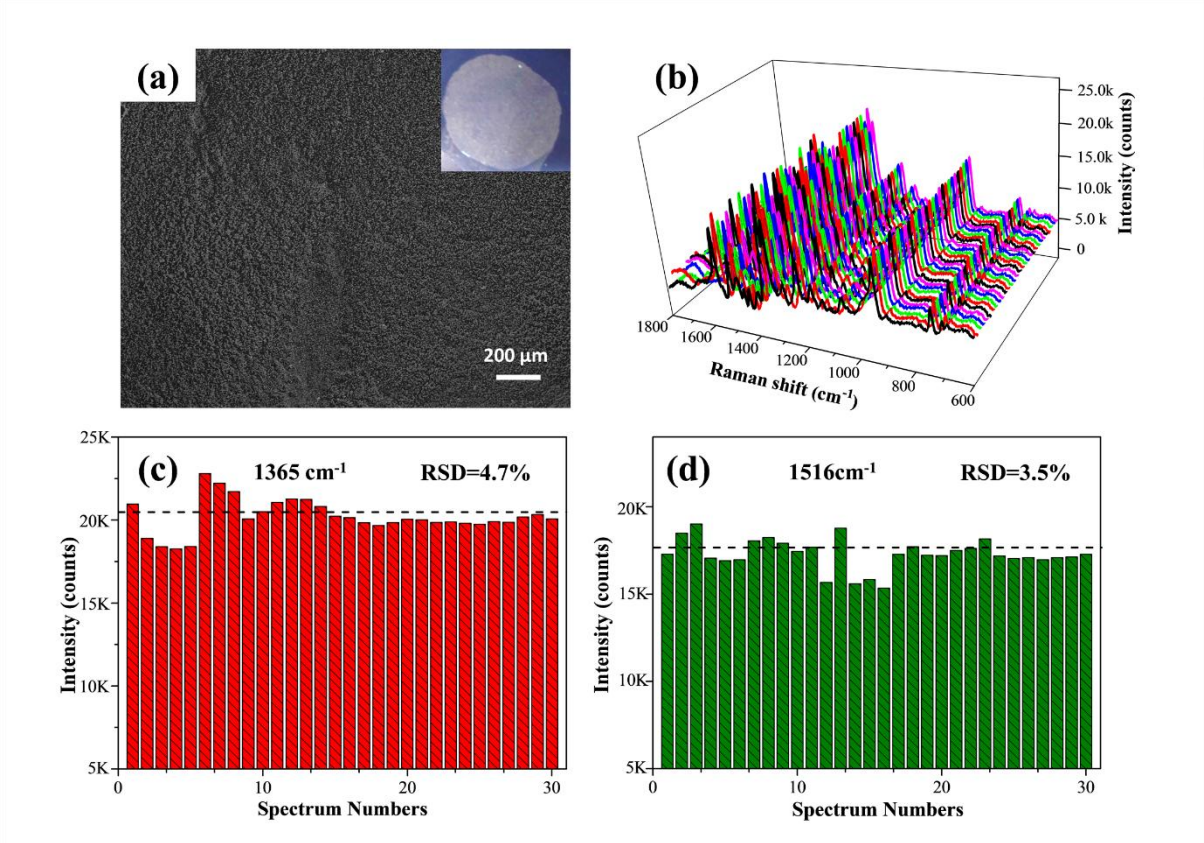

Figure 7 SERS spectra of amaranth based on spinning coating. (a) SEM images of the HAAA-NUs; (b) SERS spectra of random 30 spots; (c) and (d) The RSD values for 1365 cm^{-1} and 1516 cm^{-1} band. The inset in (a) was optical image. The concentration of probe molecule was 10-5 M

Fig 7(a) showed the SEM images of self-assembled HAAA-NUs with spin coating. .Figure S6 (a) and S6 (b) were the magnified SEM images of the HAAA-NUs. The results showed that the nanoparticles were monolayer distributed densely on the silicon wafer in a large area, which would be helpful for a uniform SERS signal. Moreover, the junction of adjacent NPs was several tens of nanometers, which would offer abundant "hot spots" during the SERS detection. The inset in Fig 7 (a) was the optical image of SERS substrate, indicating that the technique of spin coating could present the generation of "coffee ring effects" obviously. To evaluate the reproducibility of SERS signals, 30 points were selected in the whole area of the SERS substrates, and probe molecules with different concentrations

ACCEPTED

ACCEPTED MANUSCRIPT

(10^{-5} M and 10^{-6} M) were detected. For each concentration, 50 μl of aqueous amaranth solution was dropped onto the monolayer HAAA-NUs substrates. After the evaporation of solvent, Raman signals were acquired using the same detection conditions mentioned above.

Fig 7 (b) showed the 3D SERS spectra of 10^{-5} M amaranth based on spin coating process, and Fig 7(c) and 7 (d) were the intensity distributions of SERS signal at 1365 cm^{-1} and 1516 cm^{-1} peaks. The results exhibited an excellent performance of reproducibility, due to the very low RSD values of 1365 cm^{-1} band (4.7%) and 1516 cm^{-1} band (3.5%). Obviously, compared with the SERS performance based on "coffee ring effects" above, the method of spin coating showed higher reproducibility. This was much better than the 20% value reported for dried, deposited nanoparticle films.[47] In addition, Fig S7 and S8 showed the SERS performances of 10^{-6} M amaranth molecules, which also exhibited an excellent uniformity.

The ultralow RSD and excellent uniformity could be attributed to the reasons based on the self-assembled monolayer HAAA-NUs. The first reason was the uniform distribution of "hot-spots" in all regions. Both the gold tips and the junctions between neighboring NPs could enhance the intensity of the electromagnetic field, which would generate uniform dispersed SERS "hot spots" with high density. The second feature was the monolayer distribution of HAAA-NUs. Compared with the densely aggregated NPs, the monolayer colloidal NPs could avoid the steric hindrance in vertical direction[48]. During the Raman test, SERS signals would be enhanced only by the monolayer HAAA-NUs, which may leads to ultralow RSD. . Lastly, the laser spot of portable Raman system was about tens of micrometres in diameter size, and a set number of HAAA-NUs would be contained during the Raman measurement, which might be beneficial for the high uniformity and reproducibility of SERS signals.

CONCLUSIONS

ACCEPTED MANUSCRIPT

In conclusion, we have evaluated the colloidal droplets-evaporation process of colloidal nanoparticle suspensions. Combined the "coffee ring effects" with sensitive SERS analysis, the LOD of amaranth molecule could be down to 10^{-8} M. In particular, a monolayer dispersed HAAA-NUs could be obtained with the method of spin coating during the evaporation process. The RSD value of SERS signal could be as low as 3.5%, showing an improved uniformity compared to the previous studies[49-50]. The research here may be useful for optimal preparation of SERS substrates based on colloidal suspensions, and would provide simple and more sensitive SERS applications in the future.

CORRESPONDING AUTHORS

* E-mail: jxfang@mail.xjtu.edu.cn; westyx@126.com. Telephone: +86-029-82665995.

ACKNOWLEDGMENTS

This work is supported by National Natural Science Foundation of China (No 21675122) and Doctoral Fund of Ministry of Education of China (Nos. 20130201110032).

REFERENCES

(1) Fan, M.; Andrade, G. F. S.; Brolo, A. G. A Review on the Fabrication of Substrates for Surface Enhanced Raman Spectroscopy and Their Applications in Analytical Chemistry. *Analytica chimica acta.* **2011**, *693*, 7-25.

(2) Indrasekara, A. S. D. S.; Meyers, S.; Shubeita, S.; Feldman, L. C.; Gustafsson, T.; Fabris, L. Gold Nanostar Substrates for Sers-Based Chemical Sensing in the Femtomolar Regime. *Nanoscale.* **2014**, *6*, 8891.

ACCEPTED MANUSCRIPT

(3) Schlucker, S. Surface-Enhanced Raman Spectroscopy: Concepts and Chemical Applications. *Angewandte Chemie.* **2014**, *53*, 4756-95.

(4) Keskin, S.; Culha, M. Label-Free Detection of Proteins from Dried-Suspended Droplets Using Surface Enhanced Raman Scattering. *The Analyst.* **2012**, *137*, 2651-7.

(5) Tian, C., et al. Gold Mesoflower Arrays with Sub-10 Nm Intraparticle Gaps for Highly Sensitive and Repeatable Surface Enhanced Raman Spectroscopy. *Nanotechnology.* **2012**, *23*, 165604.

(6) Tian, C.; Li, J.; Ma, C.; Wang, P.; Sun, X.; Fang, J. An Ordered Mesoporous Ag Superstructure Synthesized Via a Template Strategy for Surface-Enhanced Raman Spectroscopy. *Nanoscale.* **2015**, *7*, 12318-24.

(7) Li, J. F.; Zhang, Y. J.; Rudnev, A. V.; Anema, J. R.; Li, S. B.; Hong, W. J.; Rajapandiyan, P.; Lipkowski, J.; Wandlowski, T.; Tian, Z. Q. Electrochemical Shell-Isolated Nanoparticle-Enhanced Raman Spectroscopy: Correlating Structural Information and Adsorption Processes of Pyridine at the Au(Hkl) Single Crystal/Solution Interface. *J. Am. Chem. Soc.* **2015**, *137*, 2400-2408.

(8) Liu, B.; Blaszczyk, A.; Mayor, M.; Wandlowski, T. Redox-Switching in a Viologen-Type Adlayer: An Electrochemical Shell-Isolated Nanoparticle Enhanced Raman Spectroscopy Study on Au(111)-(1×1) Single Crystal Electrodes. *ACS Nano.* **2011**, *5*, 5662-5672.

(9) Xie, W.; Walkenfort, B.; Schlücker, S. Label-Free Sers Monitoring of Chemical Reactions Catalyzed by Small Gold Nanoparticles Using 3d Plasmonic Superstructures. *J. Am. Chem. Soc.* **2013**, *135*, 1657-1660.

ACCEPTED MANUSCRIPT

(10) Formo, E. V.; Mahurin, S. M.; Dai, S. Robust Sers Substrates Generated by Coupling a Bottom-up Approach and Atomic Layer Deposition. *ACS Applied Materials & Interfaces.* **2010**, *2*, 1987-1991.

(11) Tittl, A.; Yin, X.; Giessen, H.; Tian, X.-D.; Tian, Z.-Q.; Kremers, C.; Chigrin, D. N.; Liu, N. Plasmonic Smart Dust for Probing Local Chemical Reactions. *Nano letters.* **2013**, *13*, 1816-1821.

(12) Shafer-Peltier, K. E.; Haynes, C. L.; Glucksberg, M. R.; Van Duyne, R. P. Toward a Glucose Biosensor Based on Surface-Enhanced Raman Scattering. *J. Am. Chem. Soc.* **2003**, *125*, 588-593.

(13) Yang, D.; Zhou, H.; Ying, Y.; Niessner, R.; Haisch, C. Surface-Enhanced Raman Scattering for Quantitative Detection of Ethyl Carbamate in Alcoholic Beverages. *Analytical and Bioanalytical Chemistry.* **2013**, *405*, 9419-9425.

(14) Chen, L.-M.; Liu, Y.-N. Surface-Enhanced Raman Detection of Melamine on Silver-Nanoparticle-Decorated Silver/Carbon Nanospheres: Effect of Metal Ions. *ACS Applied Materials & Interfaces.* **2011**, *3*, 3091-3096.

(15) Bell, S. E. J.; Sirimuthu, N. M. S. Rapid, Quantitative Analysis of Ppm/Ppb Nicotine Using Surface-Enhanced Raman Scattering from Polymer-Encapsulated Ag Nanoparticles (Gel-Colls). *The Analyst.* **2004**, *129*, 1032-1036.

(16) Ma, P.; Liang, F.; Diao, Q.; Wang, D.; Yang, Q.; Gao, D.; Song, D.; Wang, X. Selective and Sensitive Sers Sensor for Detection of Hg2+ in Environmental Water Base on Rhodamine-Bonded and Amino Group Functionalized Sio2-Coated Au-Ag Core-Shell Nanorods. *RSC Advances.* **2015**, *5*, 32168-32174.

ACCEPTED MANUSCRIPT

(17) Zhang, X.; Young, M. A.; Lyandres, O.; Van Duyne, R. P. Rapid Detection of an Anthrax Biomarker by Surface-Enhanced Raman Spectroscopy. *Journal of the American Chemical Society.* **2005**, *127*, 4484-4489.

(18) Xu, J.; Du, J.; Jing, C.; Zhang, Y.; Cui, J. Facile Detection of Polycyclic Aromatic Hydrocarbons by a Surface-Enhanced Raman Scattering Sensor Based on the Au Coffee Ring Effect. *ACS Applied Materials & Interfaces.* **2014**, *6*, 6891-6897.

(19) Wang, W.; Yin, Y.; Tan, Z.; Liu, J. Coffee-Ring Effect-Based Simultaneous Sers Substrate Fabrication and Analyte Enrichment for Trace Analysis. *Nanoscale.* **2014**, *6*, 9588.

(20) Barman, I.; Dingari, N. C.; Kang, J. W.; Horowitz, G. L.; Dasari, R. R.; Feld, M. S. Raman Spectroscopy-Based Sensitive and Specific Detection of Glycated Hemoglobin. *Analytical chemistry.* **2012**, *84*, 2474-82.

(21) Que, R.; Shao, M.; Zhuo, S.; Wen, C.; Wang, S.; Lee, S.-T. Highly Reproducible Surface-Enhanced Raman Scattering on a Capillarity-Assisted Gold Nanoparticle Assembly. *Advanced Functional Materials.* **2011**, *21*, 3337-3343.

(22) Liu, Z.; Cheng, L.; Zhang, L.; Jing, C.; Shi, X.; Yang, Z.; Long, Y.; Fang, J. Large-Area Fabrication of Highly Reproducible Surface Enhanced Raman Substrate Via a Facile Double Sided Tape-Assisted Transfer Approach Using Hollow Au-Ag Alloy Nanourchins. *Nanoscale.* **2014**, *6*, 2567-72.

(23) Zhang, L.; Guan, C.; Wang, Y.; Liao, J. Highly Effective and Uniform Sers Substrates Fabricated by Etching Multi-Layered Gold Nanoparticle Arrays. *Nanoscale.* **2016**, *8*, 5928-5937.

ACCEPTED MANUSCRIPT

(24) Zhao, L.; Blackburn, J.; Brosseau, C. L. Quantitative Detection of Uric Acid by Electrochemical-SurfaceEnhanced Raman Spectroscopy Using a Multilayered Au/Ag Substrate. *Anal Chem.* **2015**, *87*, 441-447.

(25) Liu, Z.; Yang, Z.; Peng, B.; Cao, C.; Zhang, C.; You, H.; Xiong, Q.; Li, Z.; Fang, J. Highly Sensitive, Uniform, and Reproducible Surface-Enhanced Raman Spectroscopy from Hollow Au-Ag Alloy Nanourchins. *Advanced materials.* **2014**, *26*, 2431-2439.

(26) Filik, J.; Stone, N. Drop Coating Deposition Raman Spectroscopy of Protein Mixtures. *The Analyst.* **2007**, *132*, 544-550.

(27) Deegan, R. D.; Bakajin, O.; Dupont, T. F.; Huber, G.; Nagel, S. R.; Witten, T. A. Capillary Flow as the Cause of Ring Stains from Dried Liquid Drops. *Nature.* **1997**, *389*, 827-829.

(28) Liu, X.; Cao, L.; Song, W.; Ai, K.; Lu, L. Functionalizing Metal Nanostructured Film with Graphene Oxide for Ultrasensitive Detection of Aromatic Molecules by Surface-Enhanced Raman Spectroscopy. *Acs Applied Materials & Interfaces.* **2011**, *3*, 2944-2952.

(29) Xie, Y.; Li, Y.; Niu, L.; Wang, H.; Qian, H.; Yao, W. A Novel Surface-Enhanced Raman Scattering Sensor to Detect Prohibited Colorants in Food by Graphene/Silver Nanocomposite. *Talanta.* **2012**, *100*, 32-37.

(30) Konrad, M. P.; Doherty, A. P.; Bell, S. E. Stable and Uniform Sers Signals from Self-Assembled Two-Dimensional Interfacial Arrays of Optically Coupled Ag Nanoparticles. *Analytical chemistry.* **2013**, *85*, 6783-9.

ACCEPTED MANUSCRIPT

ACCEPTED MANUSCRIPT

(31) Perney, N. M. B.; Baumberg, J. J.; Zoorob, M. E.; Charlton, M. D. B.; Mahnkopf, S.; Netti, C. M. Tuning Localized Plasmons in Nanostructured Substrates for Surface- Enhanced Raman Scattering. *Opt. Express.* **2006**, *14*, 847-857.

(32) Sharma, B.; Frontiera, R. R.; Henry, A.-I.; Ringe, E.; Van Duyne, R. P. Sers: Materials, Applications, and the Future. *Materials Today.* **2012**, *15*, 16-25.

(33) Kim, K.; Yoon, J. K.; Lee, H. B.; Shin, D.; Shin, K. S. Surface-Enhanced Raman Scattering of 4-Aminobenzenethiol in Ag Sol: Relative Intensity of A1- and B2-Type Bands Invariant against Aggregation of Ag Nanoparticles. *Langmuir.* **2011**, *27*, 4526-31.

(34) Valley, N.; Greeneltch, N.; Van Duyne, R. P.; Schatz, G. C. A Look at the Origin and Magnitude of the Chemical Contribution to the Enhancement Mechanism of Surface-Enhanced Raman Spectroscopy (Sers): Theory and Experiment. *The Journal of Physical Chemistry Letters.* **2013**, *4*, 2599-2604.

(35) Park, W. H.; Kim, Z. H. Charge Transfer Enhancement in the Sers of a Single Molecule. *Nano letters.* **2010**, *10*, 4040-8.

(36) Sun, J.; Bao, B.; He, M.; Zhou, H.; Song, Y. Recent Advances in Controlling the Depositing Morphologies of Inkjet Droplets. *ACS Appl Mater Interfaces.* **2015**, *7*, 28086-99.

(37) Zhang, Y.; Evans, J. R. G. Morphologies Developed by the Drying of Droplets Containing Dispersed and Aggregated Layered Double Hydroxide Platelets. *Journal of Colloid and Interface Science.* **2013**, *395*, 11-17.

(38) Zhang, Y.; Yang, S.; Chen, L.; Evans, J. R. G. Shape Changes During the Drying of Droplets of Suspensions. *Langmuir.* **2008**, *24*, 3752-3758.

ACCEPTED MANUSCRIPT

(39) Anyfantakis, M.; Baigl, D. Dynamic Photocontrol of the Coffee-Ring Effect with Optically Tunable Particle Stickiness. *Angewandte Chemie-International Edition.* **2014**, *53*, 14077-14081.

(40) Larson, R. G. Re-Shaping the Coffee Ring. *Angewandte Chemie-International Edition.* **2012**, *51*, 2546-2548.

(41) Li, T.; Wu, K.; Rindzevicius, T.; Wang, Z.; Schulte, L.; Schmidt, M. S.; Boisen, A.; Ndoni, S. Wafer-Scale Nanopillars Derived from Block Copolymer Lithography for Surface-Enhanced Raman Spectroscopy. *ACS applied materials & interfaces.* **2016**, *8*, 15668-15675.

(42) Singh, A.; Gunning, R. D.; Ahmed, S.; Barrett, C. A.; English, N. J.; Garate, J.-A.; Ryan, K. M. Controlled Semiconductor Nanorod Assembly from Solution: Influence of Concentration, Charge and Solvent Nature. *Journal of Materials Chemistry.* **2012**, *22*, 1562-1569.

(43) Anyfantakis, M.; Geng, Z.; Morel, M.; Rudiuk, S.; Baigl, D. Modulation of the Coffee-Ring Effect in Particle/Surfactant Mixtures: The Importance of Particle-Interface Interactions. *Langmuir.* **2015**, *31*, 4113-4120.

(44) Still, T.; Yunker, P. J.; Yodh, A. G. Surfactant-Induced Marangoni Eddies Alter the Coffee-Rings of Evaporating Colloidal Drops. *Langmuir.* **2012**, *28*, 4984-4988.

(45) Dugyala, V. R.; Basavaraj, M. G. Control over Coffee-Ring Formation in Evaporating Liquid Drops Containing Ellipsoids. *Langmuir.* **2014**, *30*, 8680-8686.

(46) Li, Y.-F.; Sheng, Y.-J.; Tsao, H.-K. Evaporation Stains: Suppressing the Coffee-Ring Effect by Contact Angle Hysteresis. *Langmuir.* **2013**, *29*, 7802-7811.

ACCEPTED MANUSCRIPT

(47) Wang, Y.; Chen, H.; Wang, E. Facile Fabrication of Gold Nanoparticle Arrays for Efficient Surface-Enhanced Raman Scattering. *Nanotechnology*. **2008**, *19*.

(48) Lee, W.; Lee, S. Y.; Briber, R. M.; Rabin, O. Self-Assembled Sers Substrates with Tunable Surface Plasmon Resonances. *Advanced Functional Materials.* **2011**, *21*, 3424-3429.

(49) He L, Huang J, Xu T, Chen, L., Zhang, K, Han, S. Silver, nanosheet-coated inverse opal film as a highly active and uniform SERS substrate. Journal of Materials Chemistry, **2011**, *22*,1370-1374.

(50) Liu L, Wu F, Xu D, Li, N, &Lu, N. Space confined electroless deposition of silver nanoparticles for highly-uniform SERS detection. Sensors and Actuators B: Chemical, **2017**, *255*, 1401-1406.

ACCEPTED MANUSCRIPT

ACCEPTED MANUSCRIPT

Graphical abstract

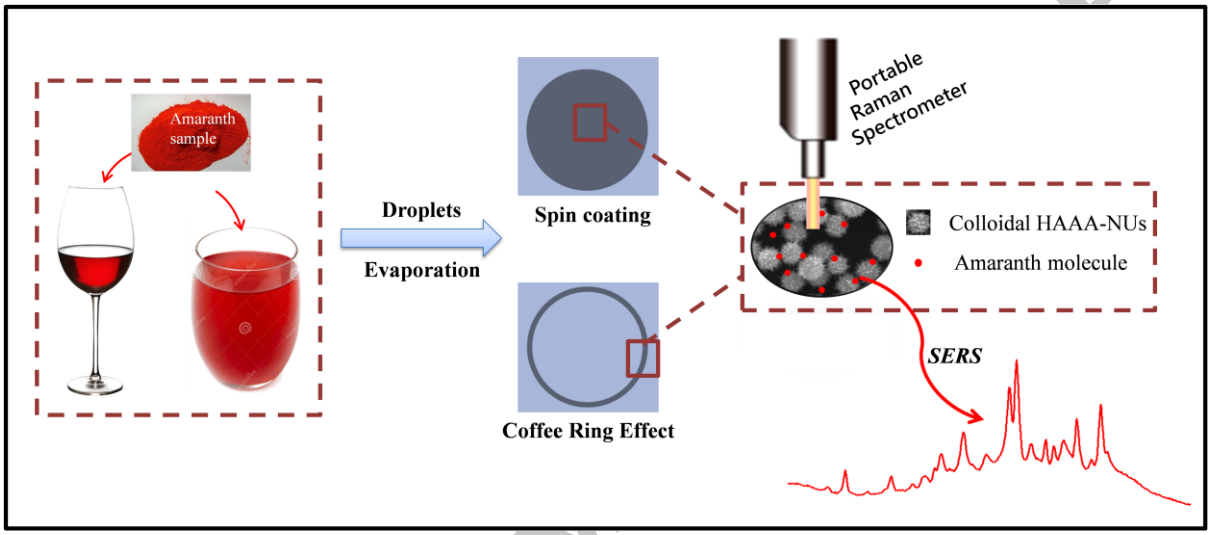

ACCEPTED MANUSCRIPT